

Radar detection of substantial presence of mid-latitude subsurface ice on Mars has been subject to a wide debate and uncertain observations. Dielectric signature of ice can be confused with other silicate rich materials. To uniquely identify ice dielectric signature, one must use the imaginary part of the dielectric constant as measured from the radar dielectric attenuation after deconvolving the scattering losses. Unfortunately the latest remains poorly quantified at both MARSIS and SHARAD frequencies. To address this ambiguity, we conducted wide-band ground penetrating radar (GPR) and resistivity investigations (ERT) in well-characterized permafrost in Fairbanks (Alaska, USA). The area shows several geomorpho-

logical and geophysical similarities to recently observed terrains in the mid- and high-latitudes of Mars [1,2,3]. The radar sounding surveys have been performed over a wide frequency range using four wide-band antennas with central frequencies of 40, 270, 400 and 900 MHz. This approach allowed us to quantify the dielectric and scattering losses mechanisms in temperate permafrost as a function of the sounding frequencies over a wide frequency band. In the light of our results, we revised the dielectric attenuation observed by SHARAD over Mid-latitude area [4,5] to obtain an accurate figure of the imaginary part of the dielectric constant and hence constrain the ambiguities associated to subsurface ice detection.

## Site Description

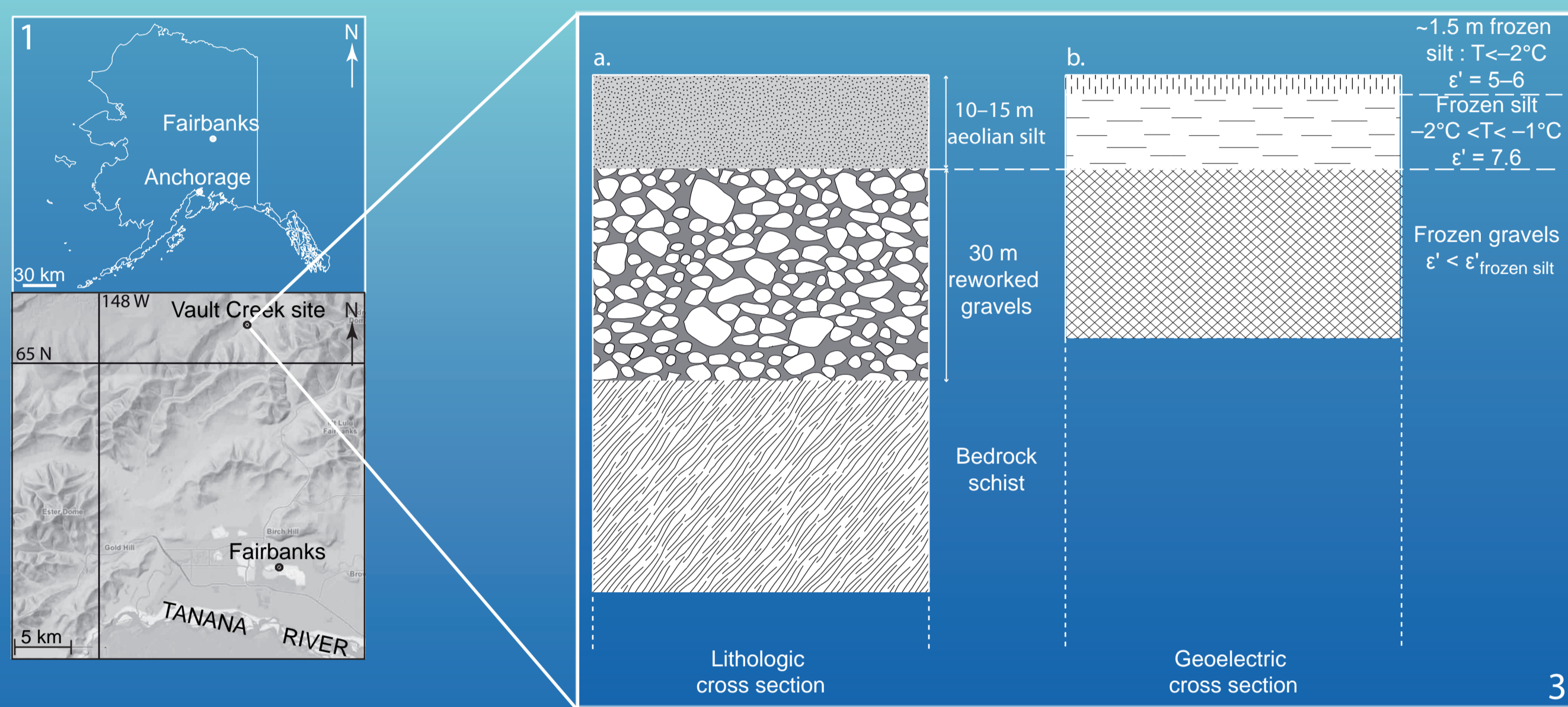


Figure 1 : Context map of Alaska and location of the investigation site (Vault Creek site), ~20 km North of Fairbanks.

Figure 2 : Average temperature versus depth profile of the Fairbanks permafrost during march 2008

Figure 3 : Lithologic (a) and geoelectric (b) cross-section of the Vault creek site subsurface. The subsurface is composed of eclogite-bearing schist amphibolites overlain by reworked creek gravels (~30 m thick) and eolian silt deposits perennially frozen with large mass of ground ice (~10 m thick) [6]. The subsurface is perennially frozen (up to ~120m deep) with large mass of ground ice (except the active layer in the upper 1 to 2 m).

## Survey results

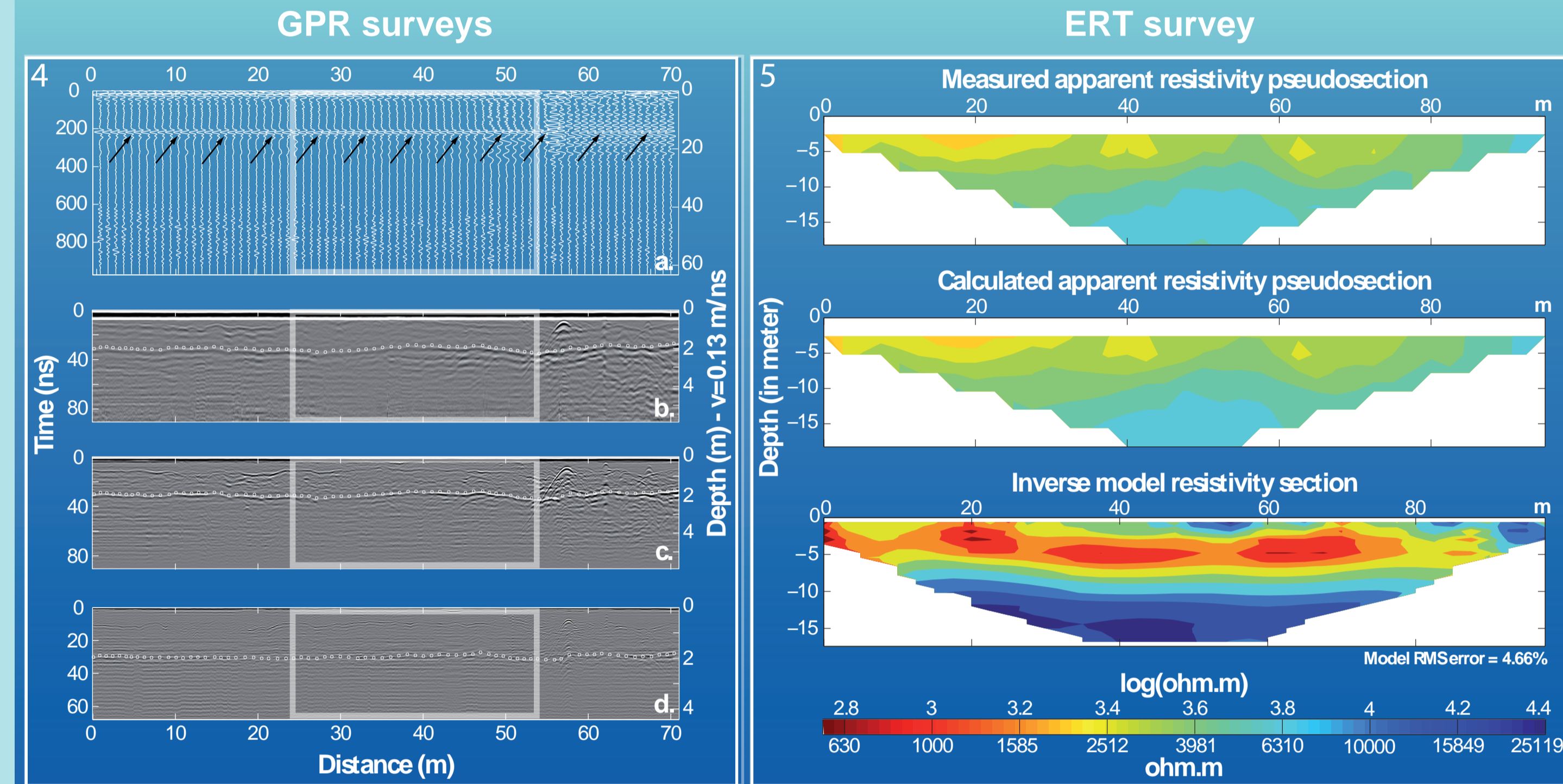


Figure 4 : (a) Radargram of the 40 MHz antenna survey (1-m interval frame). The black arrows highlight the depth of the silt/gravels interface. (b), (c), and (d) are the 270-MHz, 400-MHz and 900-MHz radargrams, respectively. The black dotted line highlights an interface where the soil temperatures are  $-2^{\circ}\text{C} < T < -1^{\circ}\text{C}$ . The gray frame on (a) and white frames on (b), (c), and (d) correspond to traces stacking used for the frequency content analysis.

Figure 5 : Measured (top) and calculated (middle) apparent resistivity pseudosections (in ohm.m) of the Wenner electrical survey (Vault creek site). The lowest pseudosection is the result of a least-square inversion of the ERT data after 8 iterations (RMS error of 4.66%). The contrast between the more conductive layer and the resistive layer (~8 to 10m deep) corresponds to the silt/gravels interface. We used the software RES2DINV (Geotomo Software [7]).

## Data processing and interpretation

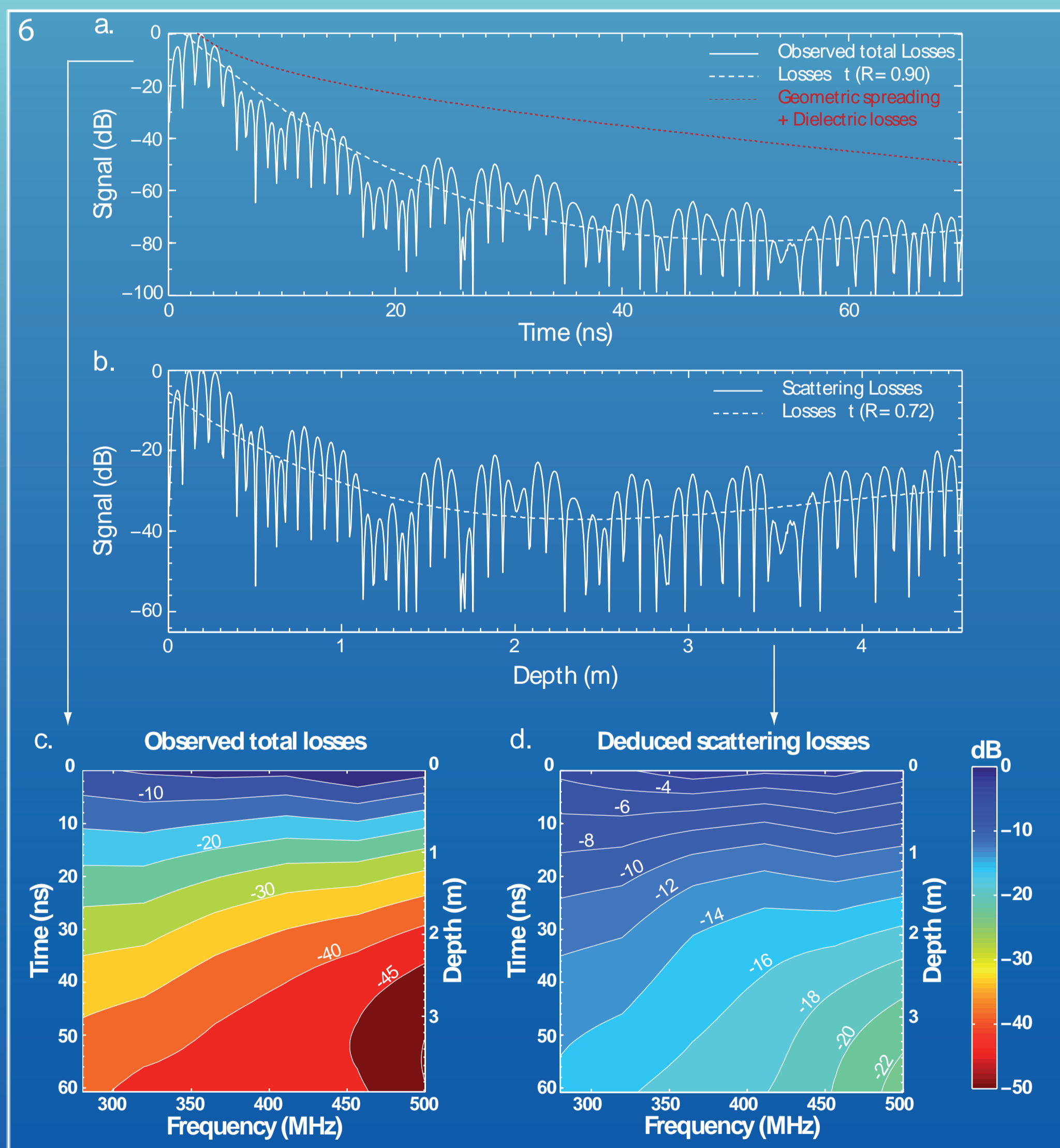


Figure 6 : Frequency-content analysis of the 400-MHz-antenna survey stacked-frame (see Fig. 4c, white frame). (a) Observed total signal losses (in decibels) versus time (in nanoseconds). The white dashed line is the polynomial fit (degree 2) of the total signal curve.  $R$  is the correlation coefficient. The red dashed line is the sum of the signal losses generated by the geometric spreading and the dielectric attenuation. (b) Deduced scattering losses obtained removing the geometric spreading and dielectric losses (red dashed line) to the observed total losses (c) Spectrogram (in decibels) of the observed total signal losses. (d) Spectrogram of the deduced scattering signal losses.

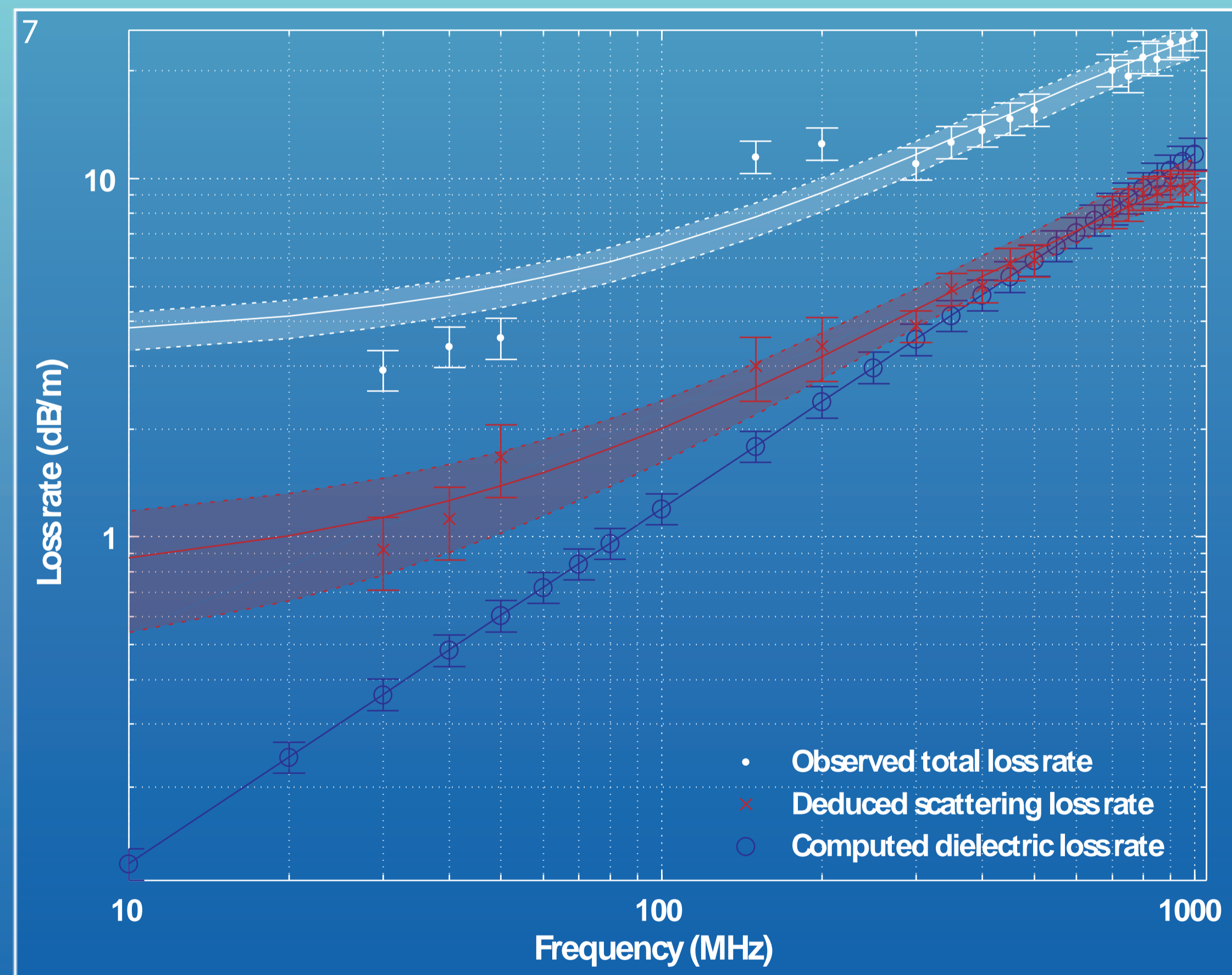


Figure 7 : Different loss rates at 3-m deep (in decibels per meter) as a function of frequency (in megahertz). White dots are observed total loss rates. Red crosses are deduced scattering loss rates. Blue circles are computed dielectric loss rate. White and red lines are the polynomial fits of the observed total loss rates and of the deduced scattering loss rates, respectively (extrapolated until 10 MHz). White and red transparent areas are delimited by the polynomial fits of the observed total loss rates and the deduced scattering loss rates, respectively, taking into account the error bars.

Loss rates deduced from observed total losses and dielectric spectrograms (Fig. 6) At 20 MHz ~70% scattering loss-rate and ~37% from [8]

	Observed loss rate not considering scattering		Considering 37% scattering losses [8]		Considering 70% scattering losses	
	$\alpha_{tot}$ (dB/m)	$\epsilon''$	$\alpha_{die}$ (dB/m)	$\epsilon''$	$\alpha_{die}$ (dB/m)	$\epsilon''$
Deuteronilus Mensae	0.026 [4]	0.012	0.016	0.008	0.008	0.004
	0.061 [5]	0.029	0.039	0.018	0.018	0.009
Amazonis Planitia	0.036 [5]	0.017	0.023	0.011	0.011	0.005
	0.058 [5]	0.028	0.036	0.017	0.017	0.010
	0.060 [5]	0.029	0.038	0.018	0.018	0.009

## References

[1] Kargel et al. (1993), Planet. Space Sci., 52, 149–156. [5] Campbell et al. (2008), JGR, 113, E12010.  
 [2] Arcone et al. (2002), JGR, 107, E11. [6] Newberry et al. (1996), AK Div. of Geol. & Geoph. Survey.  
 [3] Farr et al. (2004), Planet. Space Sci., 52, 3–10. [7] Loke and Barker (1996), Geoph. Prospect., 44, 131-152  
 [4] Plaut et al. (2009), GRL, 36, L02203. [8] Heggy et al. (2006), JGR, 111, B06S04.

## Conclusion

This approach allowed the quantification of the dielectric and scattering loss in temperate permafrost over a wide-frequency band. At 20-MHz, our results suggest an average two-way dielectric loss-rate is of  $0.24 \pm 0.02$  dB/m, whereas the corresponding average scattering loss-rate is  $1.00 \pm 0.33$ . Our results and [8] results suggest that even if Deuteronilus Mensae deposits [4] and Vasistas Borealis Formation [5] have similar real-parts, they have different imaginary parts of the dielectric constant suggesting different bulk compositions: the first is a close fit to ice-rich deposits, while the second is more consistent with low-loss volcanic deposits.